National Technical University of Athens

Bayesian Inference on Multiscale Models of Carbon-Reinforced Polymers Accelerated by Deep Neural Networks

- **A neural network-aided Bayesian identification framework for multiscale modeling of nanocomposites , Computer Methods In Applied Mechanics and Engineering, Volume 384, 1 October 2021, 113937**

S. Pyrialakos*, I. Kalogeris, G. Sotiropoulos, V. Papadopoulos

M Group

MTWIN

DIGITAL TWINS

Overview

- Multiscale model composition
- Polymer/CNT interface formulation
- Bayesian update of the interfacial properties
- Neural network-based surrogate of the RVE
- Applications / Conclusions

Multiscale model composition

PEEK polymer/ single walled CNTs armchair (8,8)

- Atomic representation of CNTs
- Connection to the nano-scale
  - RVE configuration
- Connection to the macro-scale
  - FE^2 algorithm

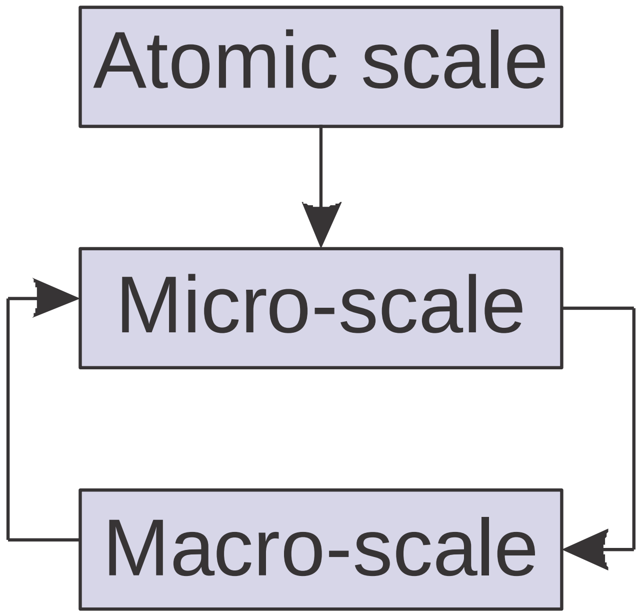

Multiscale model composition

Atomic representation of CNTs

- Carbon atom C-C bonds modeled as beams (mMSM*)
- CNT simulated as a space frame structure

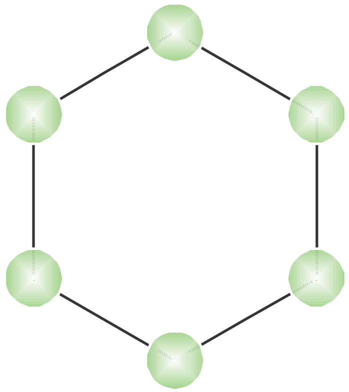

+ Accurate description

- Computational demanding

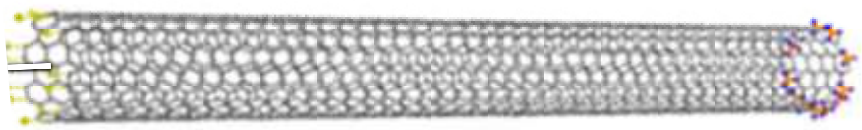

*W.-H. Chen, H.-C. Cheng, Y.-L. Liu, Radial mechanical properties of single-walled carbon nanotubes using modified molecular structure mechanics

Multiscale model composition

Connection to the micro-scale

- Each space frame is projected to an Equivalent Beam Element (EBE*)

$$(EA)_{eq} = \frac{F_x L_0}{u_x}$$

$$(EI)_{eq} = \frac{F_y L_0^3}{3u_y}$$

$$(GJ)_{eq} = \frac{T}{\varphi} L_0$$

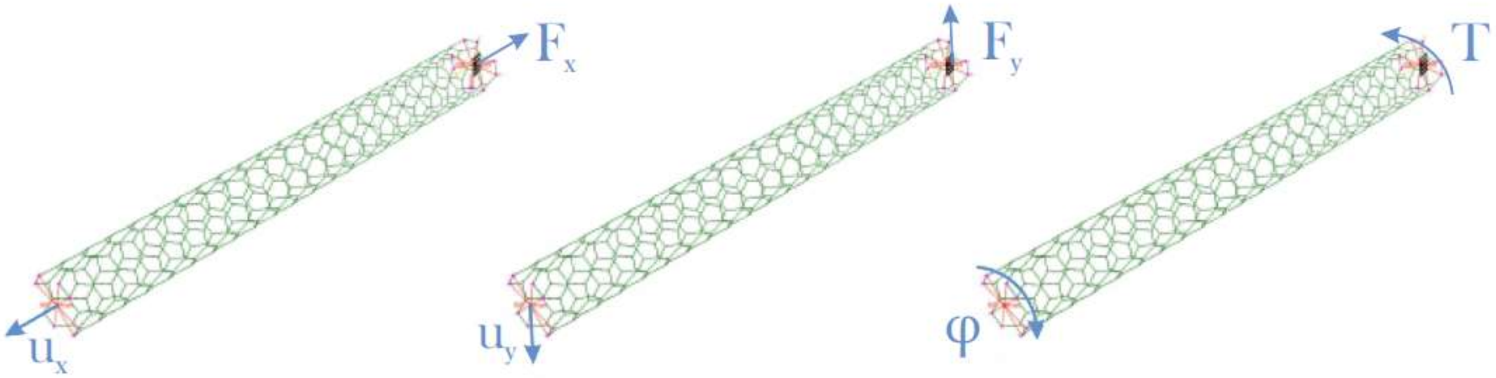

*D.N. Savvas , V. Papadopoulos, M. Papadrakakis , The effect of interfacial shear strength on damping behavior of carbon nanotube reinforced composites

Multiscale model composition

RVE configuration

1. Determine RVE dimensions

2. Add CNTs to achieve a volume fraction

3. Formulate an interaction mechanism

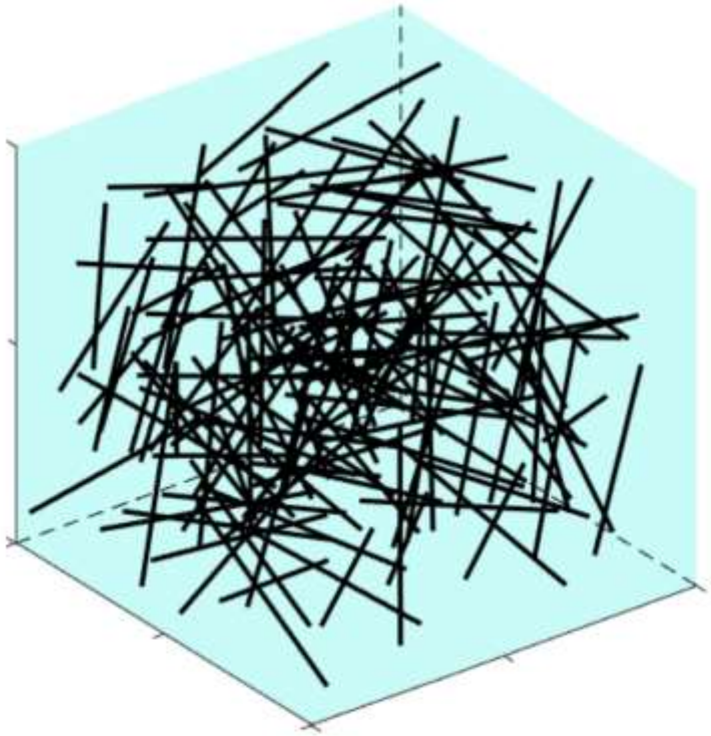

Multiscale model composition

Connection to the macro-scale

- Apply BC on RVE according to $\bar{\varepsilon}$ (localization):

$$\boldsymbol{u}(\boldsymbol{x}) = \bar{\boldsymbol{\epsilon}}\boldsymbol{x} \quad \text{at } \boldsymbol{x} \in \partial\mathcal{V}$$

- Discretize and solve RVE

- Return $\bar{\sigma}$ and $\bar{C}$ (homogenization):

$$\overline{\boldsymbol{\sigma}} = \frac{1}{\|\mathcal{V}\|}\int_{\mathcal{V}} \boldsymbol{\sigma}\, dx \qquad \overline{C} = \partial_{\bar{\epsilon}}\overline{\boldsymbol{\sigma}}$$

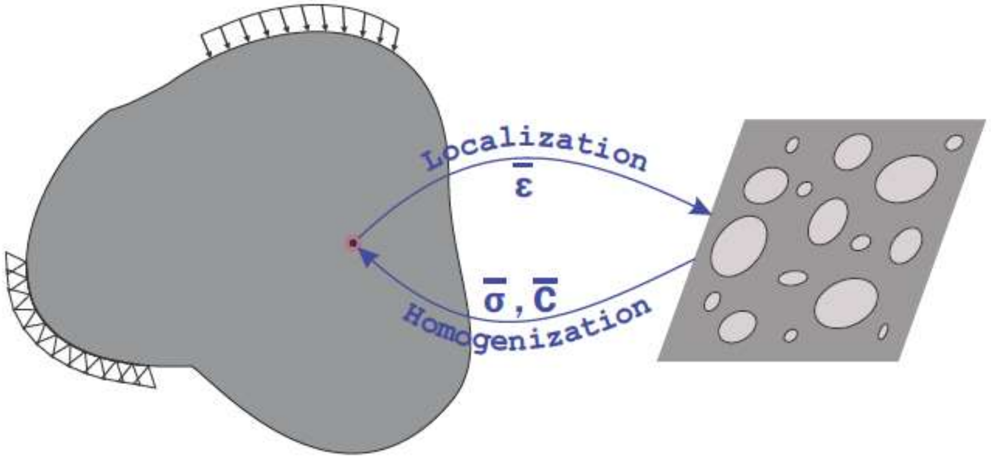

*C. Miehe, A. Koch, Computational micro-to-macro transitions of discretized microstructures undergoing small strains

Multiscale model composition

FE^2 algorithm*

+ Ideal for simulating nonlinear phenomena

- Very expensive computationally

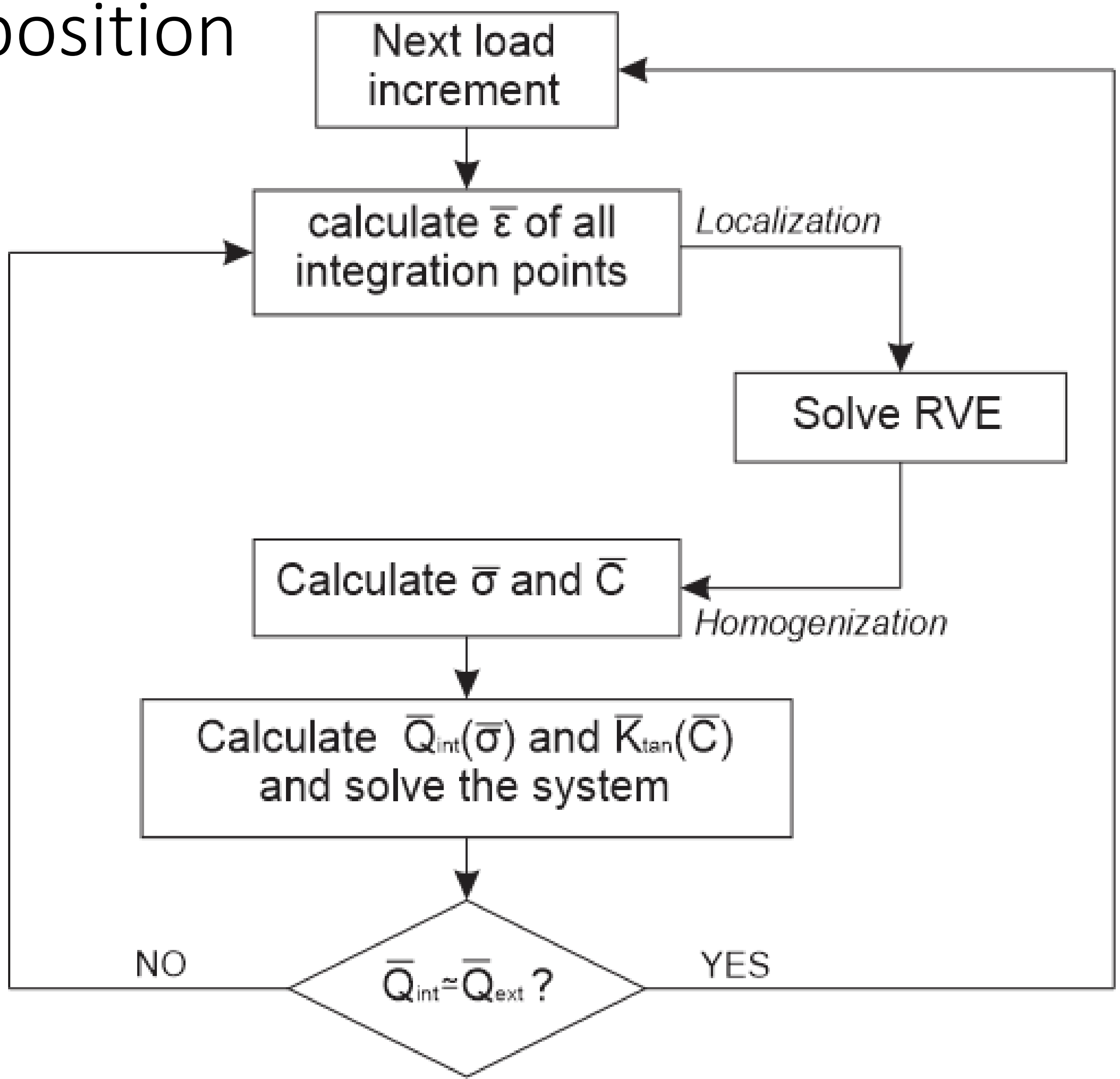

*F.Feyel , A multilevel finite element method (FE2) to describe the response of highly non-linear structures using generalized continua

Polymer/CNT interface formulation

Cohesive zone model

Relates the DOFs of the EBE with the Cohesive Beam Element (CBE)

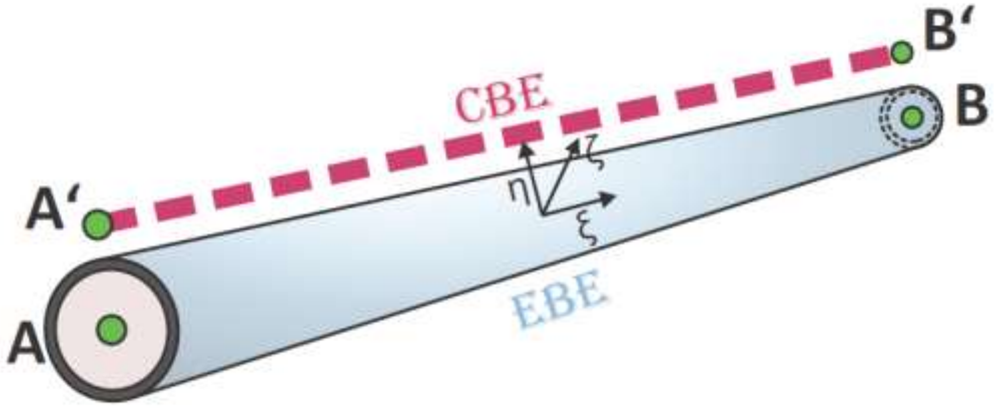

Polymer/CNT interface formulation

Embedding technique

CBE DOFs are described in terms of the surrounding matrix element's DOFs with an embedding technique

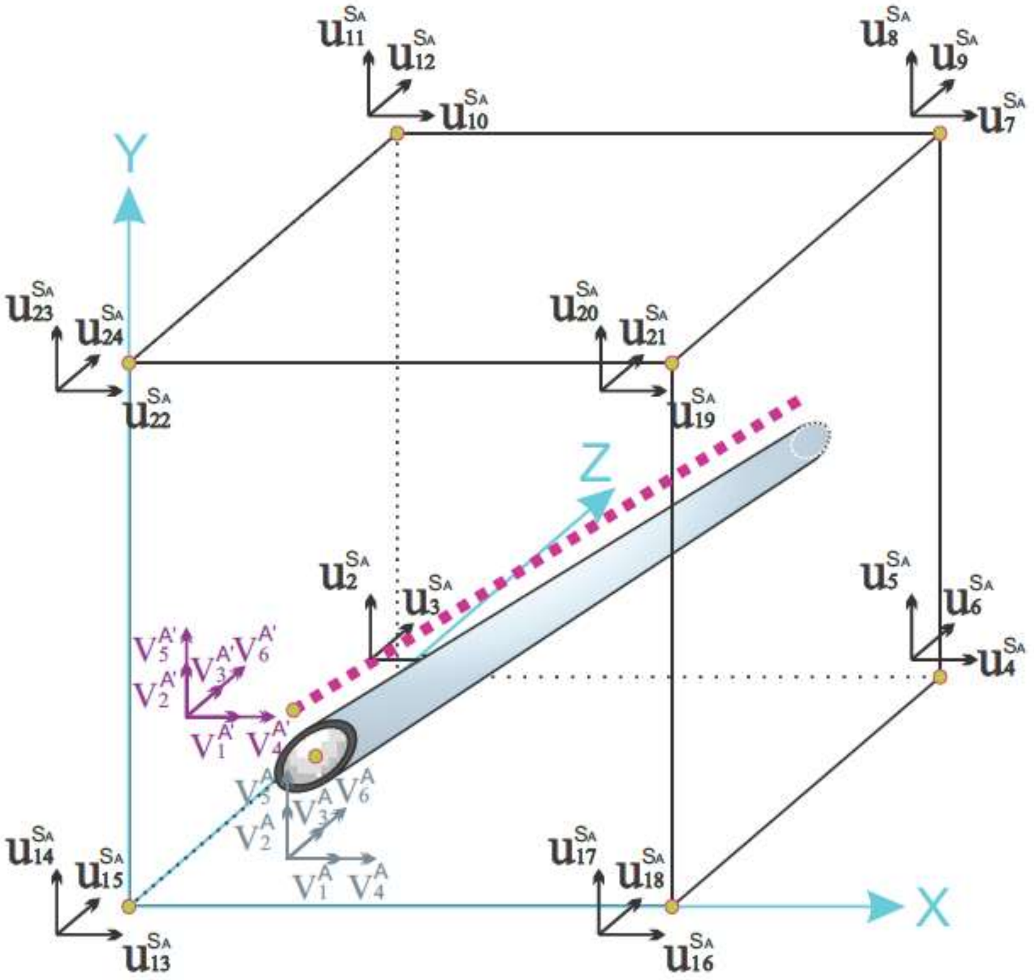

Polymer/CNT interface formulation

Interfacial constitutive law

- A bilinear bond-slip approach is selected for the slip component of the interface:

$$D_{11} = \begin{cases} D_{el}, & \tau_1 \leq \tau_{1,y} \\ D_{pl} = pD_{el}, & \tau_1 > \tau_{1,y} \end{cases}$$

$\tau_{1,y}$ → interfacial shear strength

D_{el} → elastic slope

D_{pl} → plastic slope

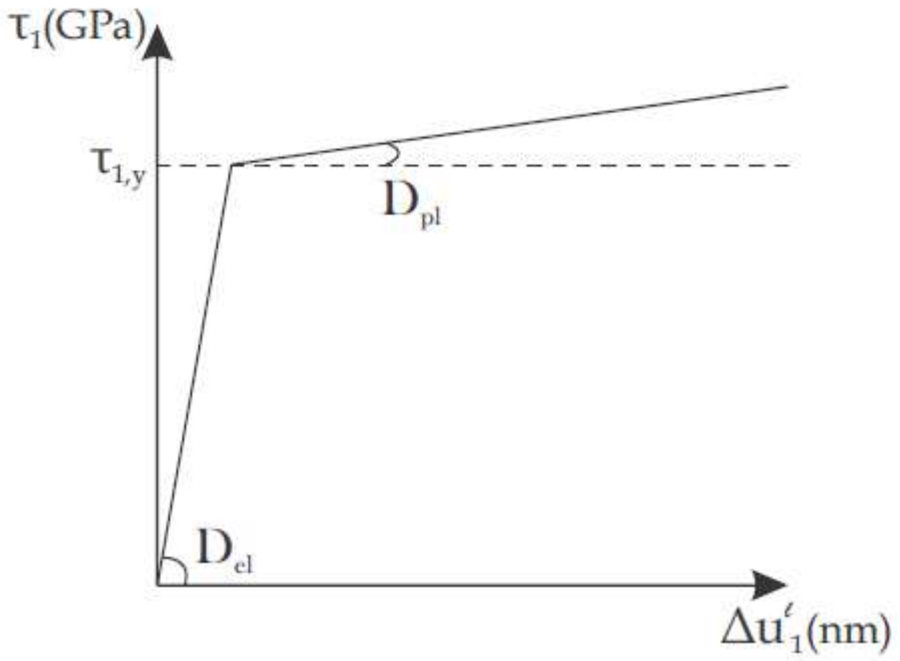

Bayesian update of the interfacial properties

Bayes Theorem:

$$\pi_{post}(\theta|\omega) = \frac{\pi(\omega|\theta)\pi_{prior}(\theta)}{\int_{-\infty}^{\infty}\int_{-\infty}^{\infty}...\int_{-\infty}^{\infty}\pi(\omega|\theta)\pi_{prior}(\theta)d\theta_1 d\theta_2...d\theta_n}$$

$\pi_{prior}(\theta)$ → Prior distribution (Prior beliefs on the probabilistic model)

$\pi(\omega|\theta)$ → Likelihood function (Relation of observations with outcomes of the model)

$\pi_{post}(\theta|\omega)$ → Posterior distribution (Updated probabilistic model)

Bayesian update of the interfacial properties

Likelihood function has the form:

$$\pi(\omega|\theta) = \pi_\epsilon(\omega - M(\theta))$$

- θ → interfacial parameters $(\tau_{1,y}, D_{el}, D_{pl})$
- ω → measurements of deformations
- $M(\theta)$ → FE^2 model predictions for given θ
- ϵ → deviation due to measurement and model errors

Bayesian update of the interfacial properties

To efficiently draw samples from the posterior distribution the Markov Chain Monte Carlo (MCMC) technique is employed with the form of the Metropolis Hastings (MH) algorithm.

The evaluation of the likelihood requires a FE^2 solution for each candidate sample $\boldsymbol{\theta}'$.

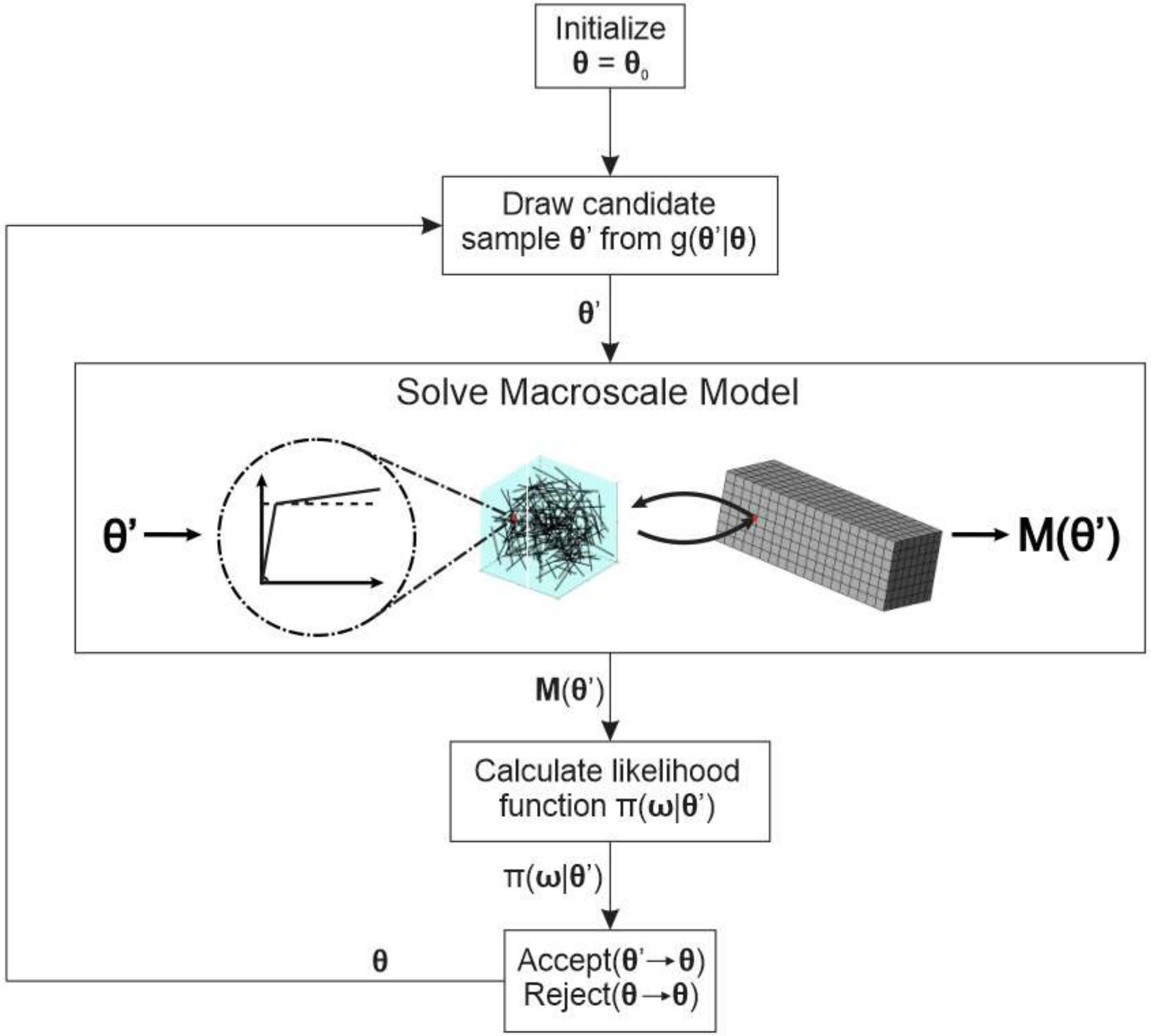

Neural network-based surrogate of the RVE

The intention is to learn the nonlinear equation of the RVE's homogenization scheme.

A Feed Forward Neural Network (FFNN) is deployed.

Input neurons consist of θ and $\bar{\varepsilon}$ while output neurons of $\bar{\sigma}$.

Appropriate selection of the ranges from which the sampling will occur.

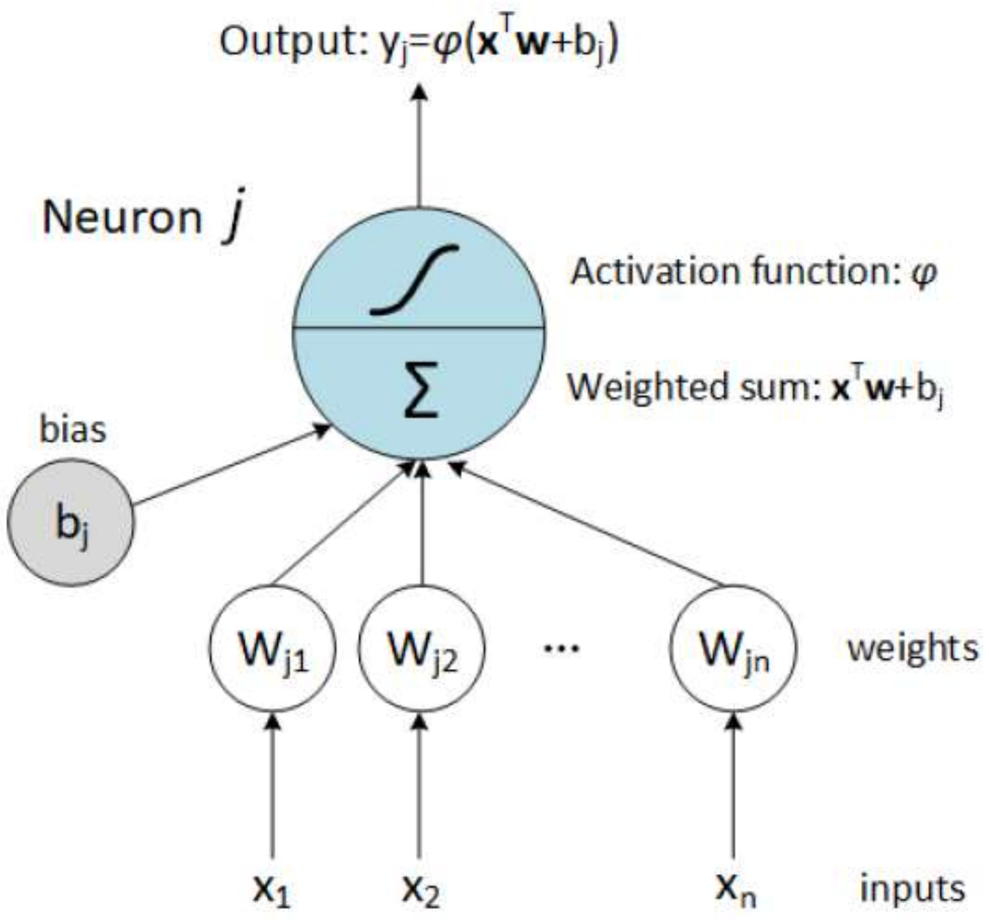

Neural network-based surrogate of the RVE

Procedure by steps:

1. Generate N random input samples within some specified ranges

2. Solve the nonlinear equation of the RVE for each input vector and get the respective output

3. Choose the FFNN architecture and train it using the N pairs of input – output.

4. Calculate $\overline{\boldsymbol{C}} = [\bar{c}_{ij}]$ using the chain rule $\bar{c}_{ij} = \frac{\partial \overline{\sigma}_{ij}}{\partial h_k} \frac{\partial h_k}{\partial h_{k-1}} \cdots \frac{\partial h_1}{\partial \overline{\epsilon}_{ij}}$, where h_k is the k_{th} hidden layer (Automatic Differentiation).

Neural network-based surrogate of the RVE

Offline procedure

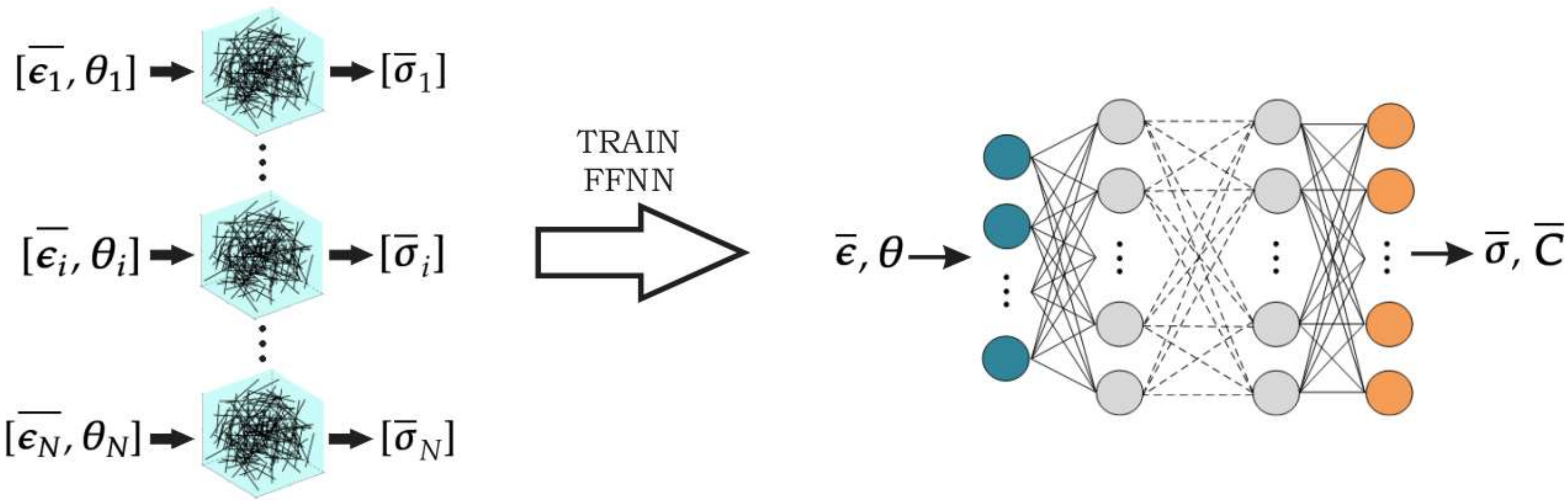

Neural network-based surrogate of the RVE

Online procedure

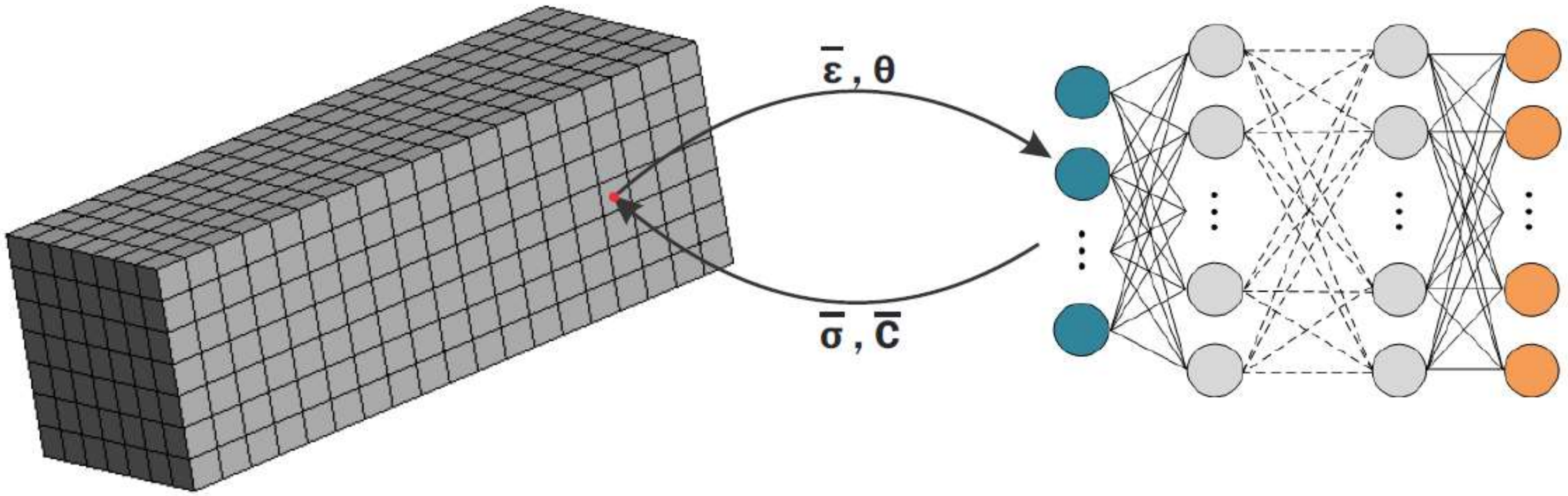

Applications

First example (2D)

A fixed composite panel made of PEEK/SWCNT is subjected to a bending test.

E=4GPa , ν=0.4

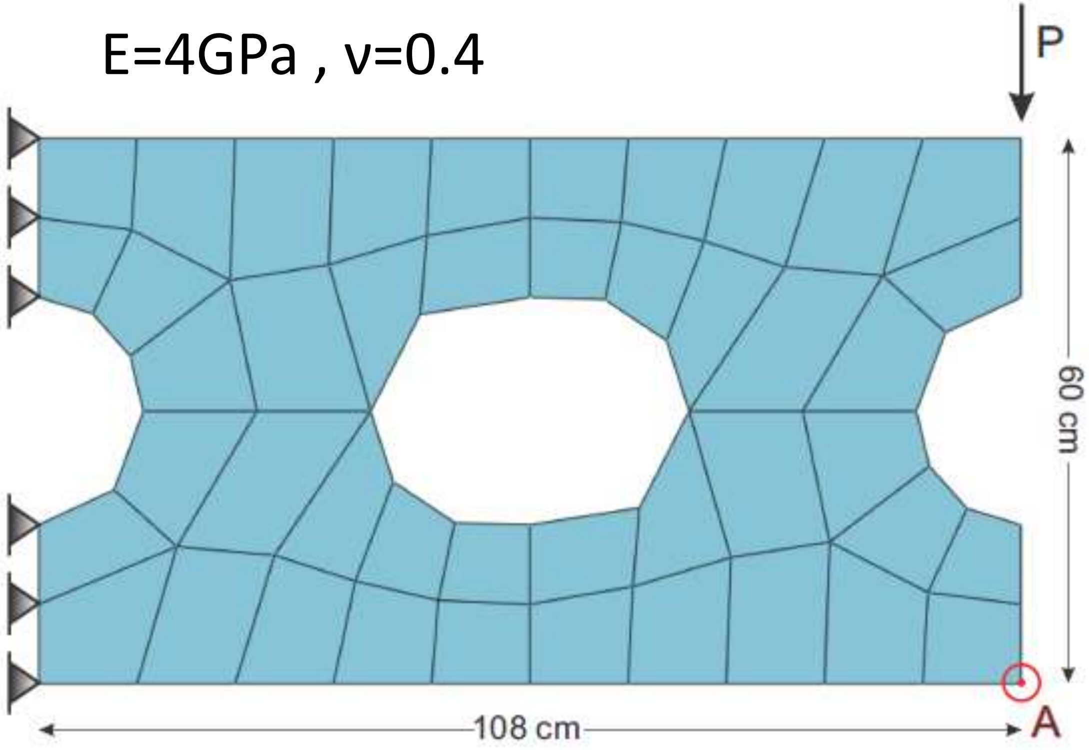

44 quadrilateral plane stress FE

P=100kN → u_A=4.2cm

Applications

2D RVE representation

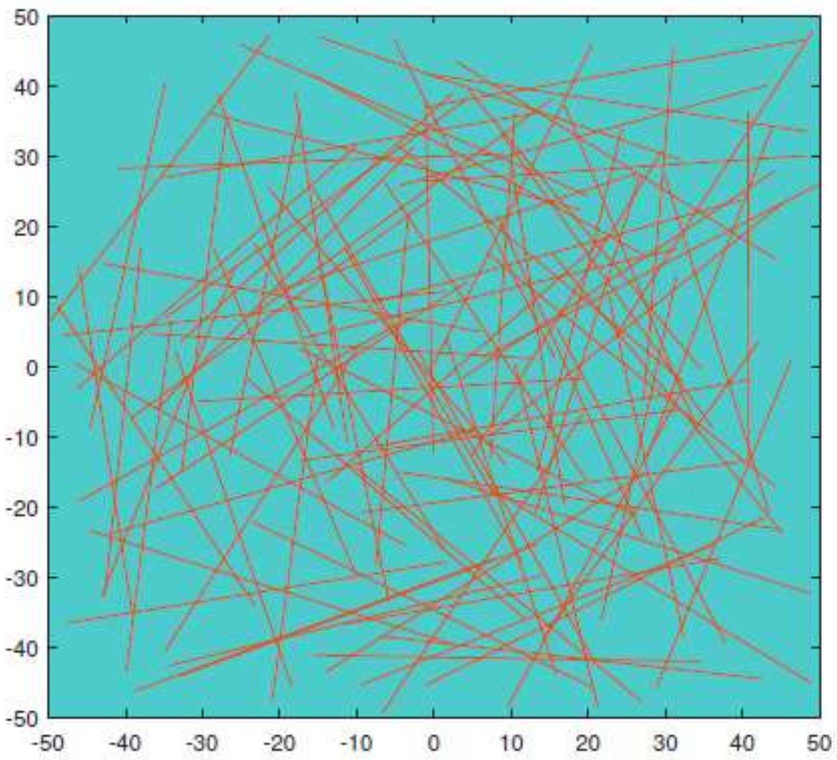

RVE dimensions 100x100x20

volume fraction 3%

CNT length L_0=50nm

EA_{eq}=694.77nN , EI_{eq}=100.18nN , GJ_{eq}=68.77GPA nm/rad

100 quadrilateral plane stress FE

Prior distributions

D_{el} - N(10,2) (GPa/nm)

D_{pl} - N(1,0.2) (GPa/nm)

$\tau_{1,y}$ - N(0.1,0.02) (GPa)

Applications

	ϵ_{11} [$-$]	ϵ_{12} [$-$]	ϵ_{22} [$-$]	D_{el} [GPa/nm]	D_{pl} [GPa/nm]	$\tau_{1,y}$ [GPa]
min	-0.1	-0.1	-0.1	1	0.1	0.01
max	0.1	0.1	0.1	20	2	0.2

Input sample ranges for the FFNN training

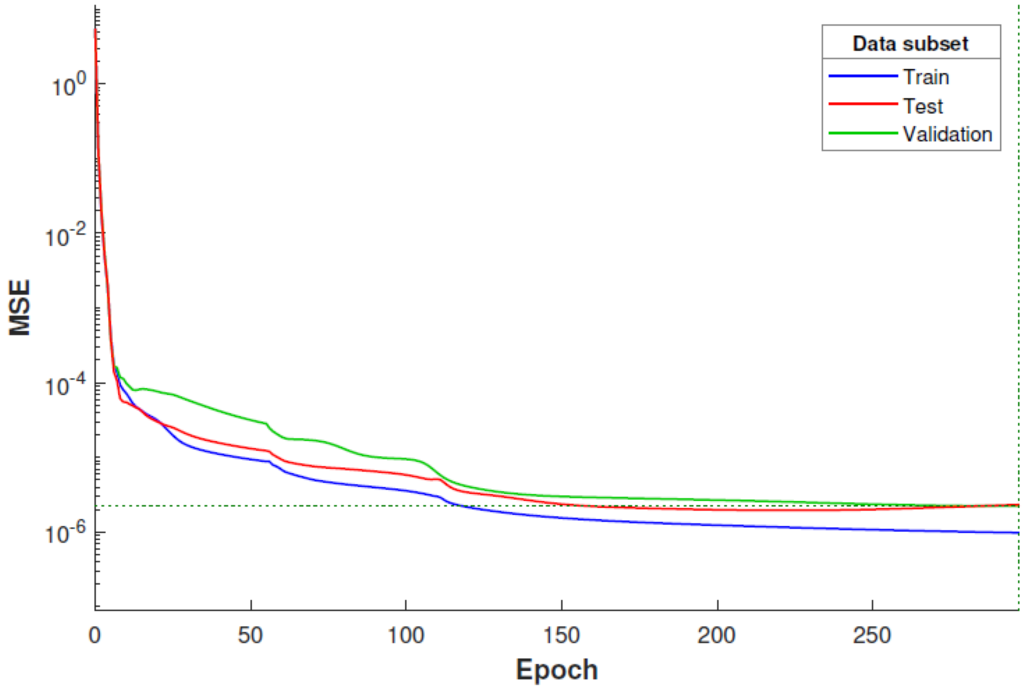

Progression of the FFNN training process

3 hidden layers

20 neurons per layer

Levenberg-Marquardt algorithm

3000 samples for FFNN train

Applications

Bayesian update was performed on both full-scale and surrogate model.

	Computational time (sec)						
	Offline		Online				Total
Model	FFNN sampling	FFNN training	RVE solution	FFNN call/ $\overline{\boldsymbol{C}}$	FE^2	MCMC	
Full scale	-	-	0.022	-	30.5	680850	680850 (189hours)
Surrogate	174	31	-	8e-5	0.115	2588	2793 (0.8hours)

Computational time of each stage of the algorithm

Applications

Bayesian update was performed on both full-scale and surrogate model.

22500 likelihood evaluations

15000 accepted samples

65% acceptance ratio

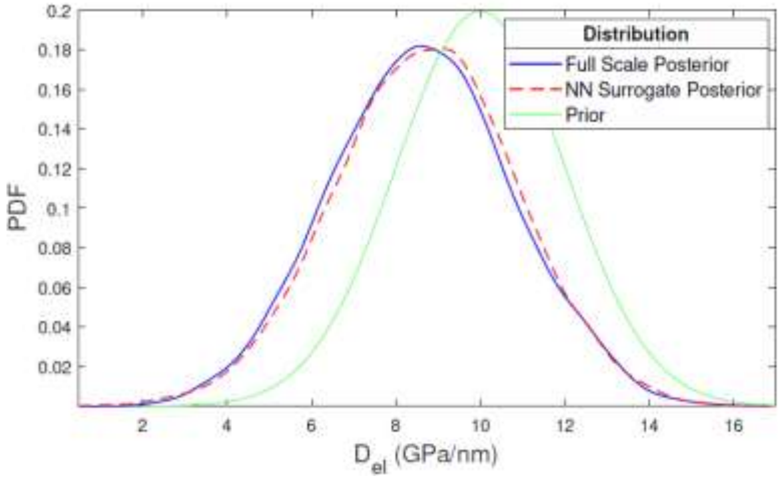

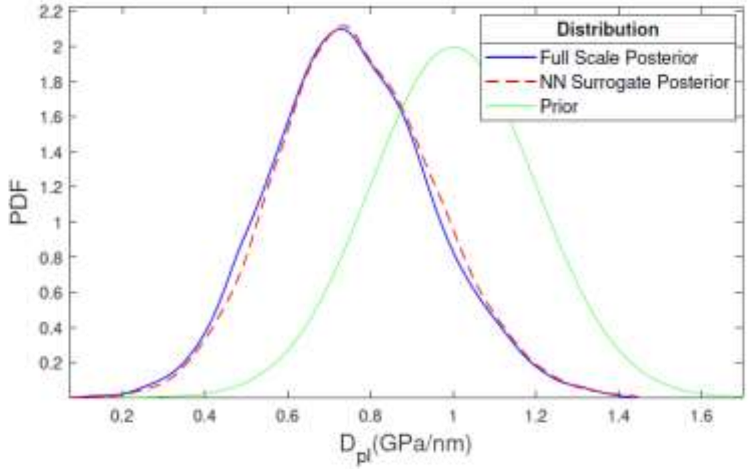

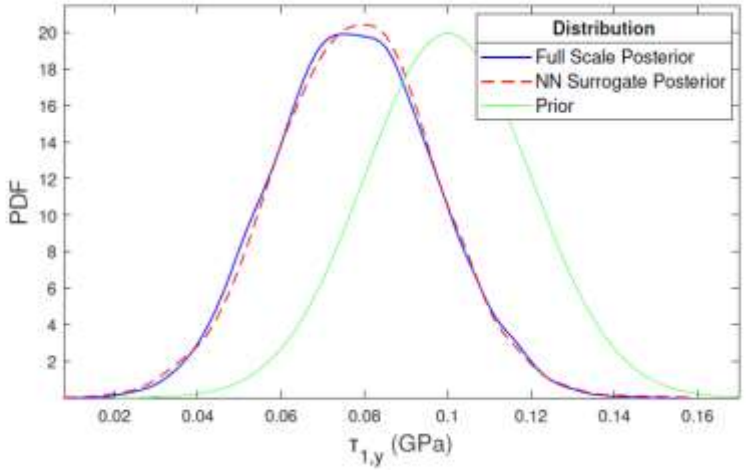

Posterior distributions for both solutions

Applications

Second example (3D)

A composite wrench fixed on the blue area while subjected to a pressure load on the purple area is studied.

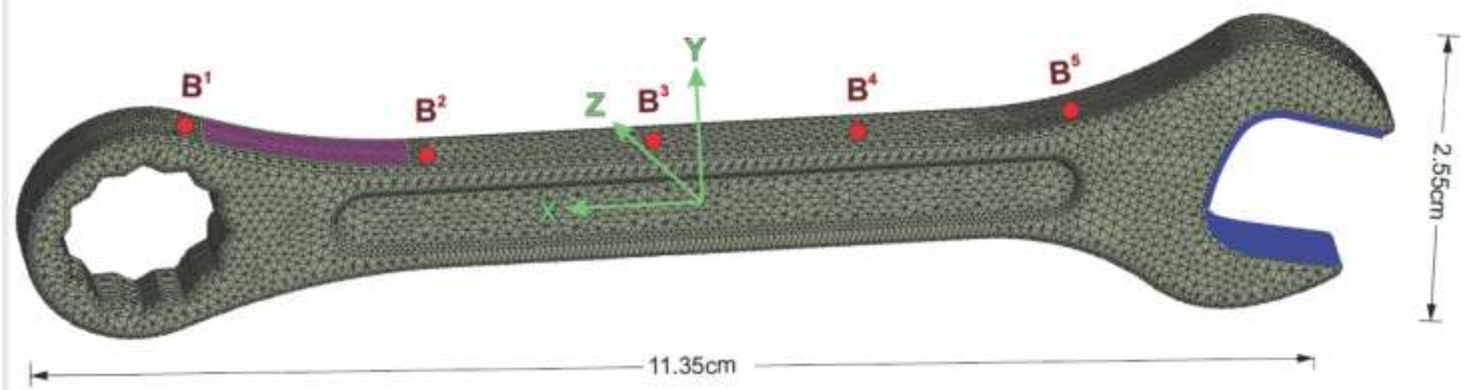

50000 tetrahedral FE

L1= 150kPa , L2=300kPa

Gaussian kernel

$$K(s) = \epsilon^2 exp\frac{(-|s|)}{\alpha}$$

Loading case	Measurement(mm)				
	B^1	B^2	B^3	B^4	B^5
L_1	-0.15	-6.50	-5.31	-4.35	-5.23
L_2	-0.31	-13.51	-11.03	-9.04	-10.88

Applications

3D RVE representation

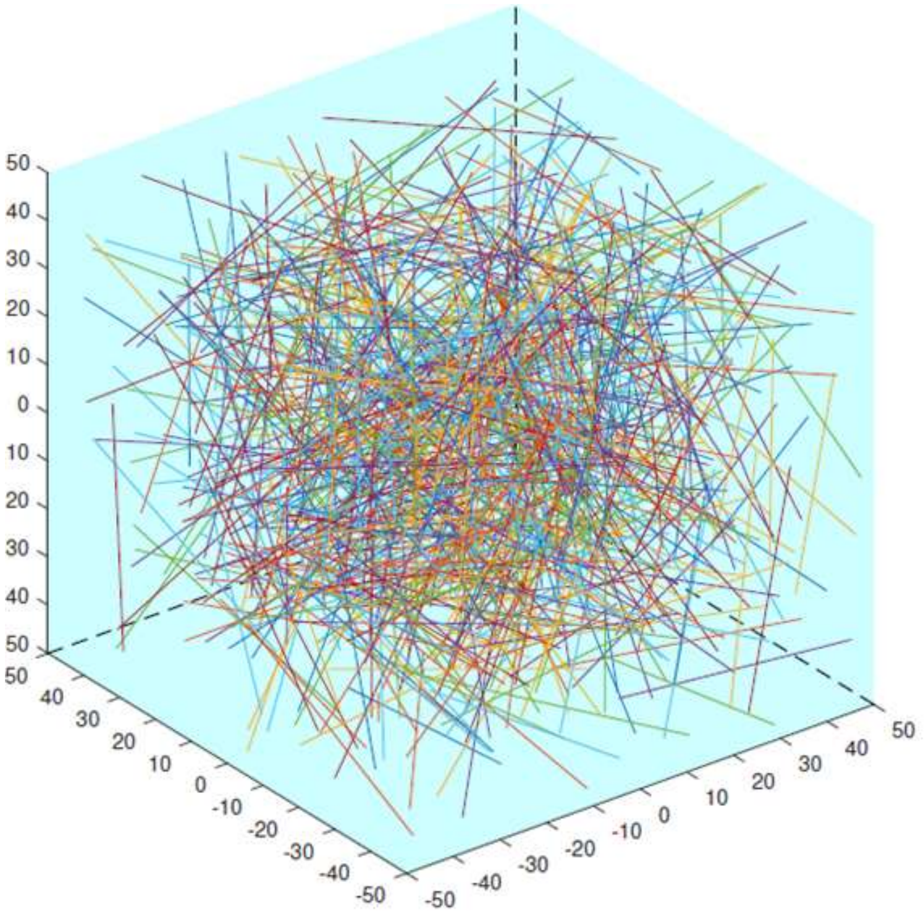

RVE dimensions 100x100x100
volume fraction 4.5%
CNT length L_0=50nm
EA_{eq}=694.77nN , EI_{eq}=100.18nN , GJ_{eq}=68.77GPA nm/rad
1000 hexagonal FE

<u>Prior distributions</u>

D_{el} - N(10,2) (GPa/nm)
D_{pl} - N(1,0.2) (GPa/nm)
$\tau_{1,y}$ - N(0.1,0.02) (GPa)

Applications

	ϵ_{11} [–]	ϵ_{12} [–]	ϵ_{13} [–]	ϵ_{22} [–]	ϵ_{23} [–]	ϵ_{33} [–]	D_{el} [GPa /nm]	D_{pl} [GPa /nm]	$\tau_{1,y}$ [GPa]
min	-0.08	-0.04	-0.04	-0.08	-0.04	-0.04	0.1	0.01	0.001
max	0.08	0.04	0.04	0.08	0.04	0.04	20	2	0.2

Input sample ranges for the FFNN training

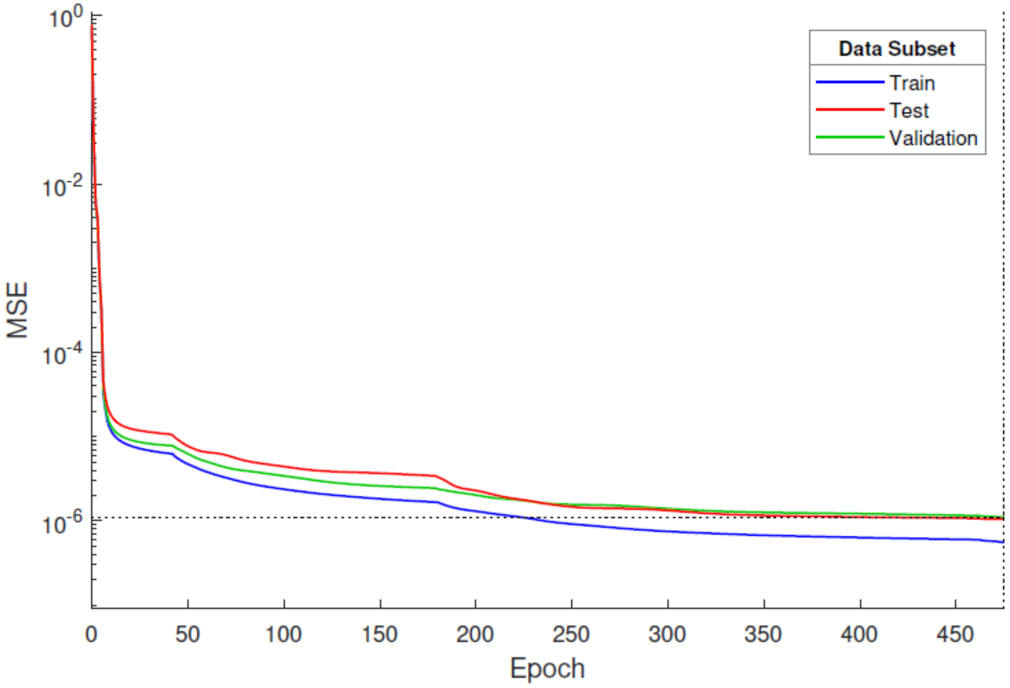

Progression of the FFNN training process

3 hidden layers 20 neurons per layer Levenberg-Marquardt algorithm
3000 samples for FFNN train

Error measurement with L_2 norm

$$err_{\overline{\boldsymbol{C}}} = \frac{\sum_{j=1}^{1000} \left\| \overline{\boldsymbol{C}}^{sur} - \overline{\boldsymbol{C}}^{FEM} \right\|_2}{\sum_{j=1}^{1000} \left\| \overline{\boldsymbol{C}}^{FEM} \right\|_2} = 1.76\%$$

$$err_{\overline{\boldsymbol{\sigma}}} = \frac{\sum_{j=1}^{1000} \left\| \overline{\boldsymbol{\sigma}}^{sur} - \overline{\boldsymbol{\sigma}}^{FEM} \right\|_2}{\sum_{j=1}^{1000} \left\| \overline{\boldsymbol{\sigma}}^{FEM} \right\|_2} = 0.80\%$$

Applications

Bayesian update was performed only on the surrogate model.

	Computational time (hours)						
	Offline		Online				Total
	FFNN sampling	FFNN training	RVE solution	FFNN call/ $\overline{\boldsymbol{C}}$	FE^2	MCMC	
Full scale (Prediction)	-	-	0.033	-	37076	926909667	926909667 (105812 years)
Surrogate	9.83	0.07	-	2.2e-8	0.014	350	359.9 (15days)

Computational time of each stage of the algorithm

Applications

Bayesian update was performed only on the surrogate model.

25000 likelihood evaluations
15000 accepted samples
60% acceptance ratio

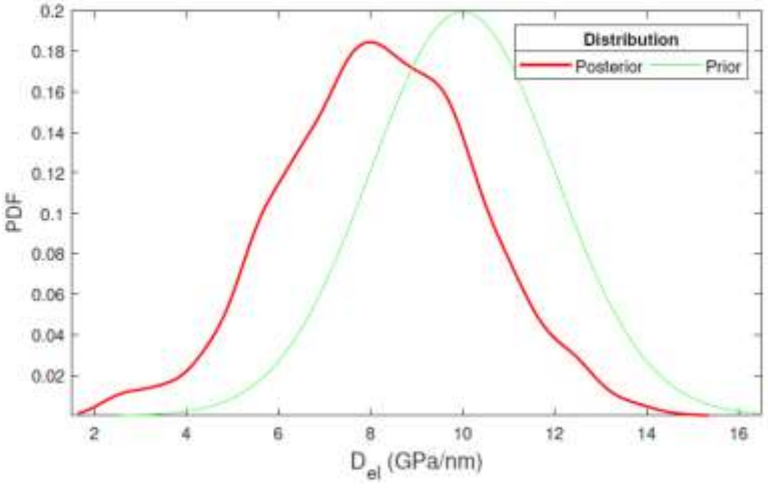

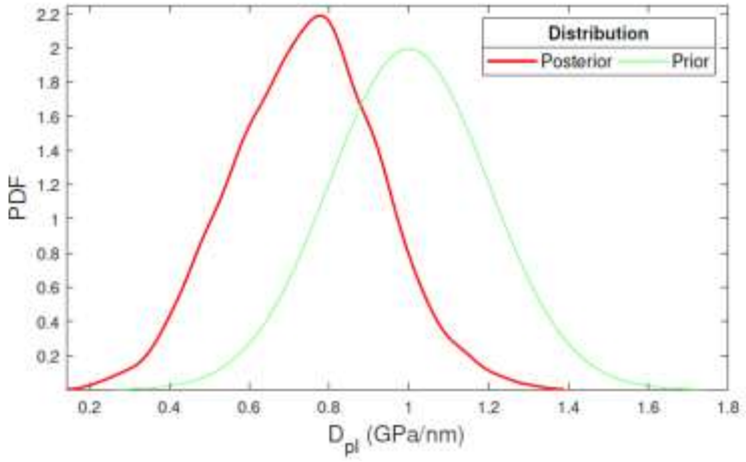

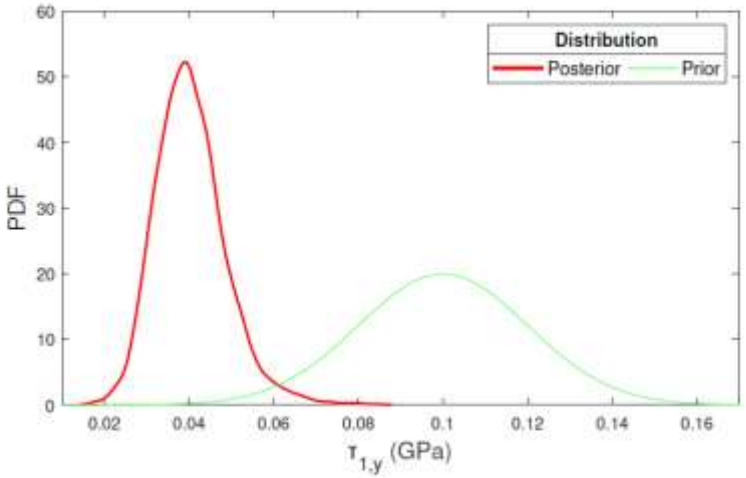

Posterior distributions for both solutions

Conclusions

- A methodology for updating the beliefs of microscale properties, which are expensive and hard to be directly measured, has been developed.

- The surrogate model displayed a high level of accuracy compared to the full-scale solution, as well as a remarkable cost reduction.

- This framework is generic and can be extended to other physically analogous phenomena.

Acknowledgements

This research has been co-financed by the European Regional Development Fund of the European Union and Greek national funds through the Operational Program Competitiveness, Entrepreneurship and Innovation, under the call RESEARCH-CREATE-INNOVATE (project code: T2EDK-03473).

This research has been co-financed by the European Regional Development Fund of the European Union and Greek national funds through the Operational Program Competitiveness, Entrepreneurship and Innovation, under the call RESEARCH-CREATE-INNOVATE (project code: T1EDK-04320).

European Union
European Regional Development Fund

EPAnEK 2014–2020
OPERATIONAL PROGRAMME
COMPETITIVENESS • ENTREPRENEURSHIP • INNOVATION

ΕΣΠΑ
2014-2020
ανάπτυξη - εργασία - αλληλεγγύη
Partnership Agreement
2014 - 2020